PCCP

Accepted Manuscript

ROYAL SOCIETY OF CHEMISTRY

www.rsc.org/pccp

Amplification of Light Collection in Solid-State Dye-Sensitized Solar Cells via Antenna Effect through Supramolecular Assembly†

Bilel Louahem M'Sabah,[1] Mourad Boucharef,[1,2] Julien Warnan,[3] Yann Pellegrin,[3] Errol Blart,[3] Bruno Lucas,[1] Fabrice Odobel,[3,*] J. Bouclé[1,*]

[1] XLIM UMR 7252, Université de Limoges/CNRS, 123 Avenue Albert Thomas, 87060 Limoges Cedex, France

[2] Université de Constantine 1, B.P. 325, Raoute Ain El Bey, Constantine 25017, Algérie

[3] UNAM, Université Nantes, Angers, UMR CNRS 6230, 2, rue de la Houssinière - BP 92208, 44322 Nantes Cedex 3, France

* Corresponding authors: johann.boucle@unilim.fr (+33587506762)
fabrice.odobel@univ-nantes.fr (+33251125429)

† Electronic supplementary information (ESI) available: Steady-state and transient photoluminescence spectra, Optical density of devices.

Abstract. This study demonstrates that the concept of molecular antenna is a relevant strategy to improve the power conversion efficiency of solid-state dye-sensitized solar cells by extending their spectral sensitivity over a broad region of the solar spectrum. In this work, we have associated a BODIPY antenna to a bi-chromophoric sensitizer made of a squaraine linked to a zinc prophyrin by axial ligation onto the zinc. Using steady-state and transient photoluminescence spectroscopy, we demonstrate that efficient energy transfers occur from the antenna to the dyad, extending its visible photosensitivity. We also show that direct electron injection from the antenna to TiO_2 is possible. A drastic improvement in device performance by a factor of three is observed under illumination using the spiro-OMeTAD molecular glass as solid-state electrolyte, leading to a panchromatic response of the device. The influence of the solid-state hole transporter on the supramolecular assembly is also discussed.

Keywords: solid-state dye-sensitized solar cells, antenna, resonant energy transfers, supramolecular assembly, spiro-OMeTAD

1. Introduction

Solid-state dye-sensitized solar cells (ssDSSC) show a great interest due to their potential low cost fabrication and relatively high efficiencies.[1] In this class of solar cells, a nanocristalline TiO_2 electrode is sensitized to visible light by a dye monolayer and infiltrated by a solid-state electrolyte, which acts as a hole transporter medium (HTM). The most efficient system is based on a push-pull organic sensitizer coded Y123 and the 2,2',7,7'-tetrakis(N,N-di-p-methoxyphenylamine)-9,9'-spirobifluorene (spiro-OMeTAD) doped with a cobalt complex as HTM, leading to a power conversion efficiency of 7.2%.[2] Alternatives HTM, including organic[3-5] and inorganic compounds,[6, 7] have been also used, the most efficient report being associated with the use of a p-type direct bandgap perovskite-like semiconductor $CsSnI_3$ that achieves efficiencies up to 8.5% with a classical ruthenium dye.[8] Additionally, major breakthroughs have recently been reported by using hybrid lead halide perovskite sensitizers such as $CH_3NH_3PbI_3$,[9] pushing the efficiencies of the ssDSSC concept close to the 20% threshold.[10] However, as promising as perovskite absorbers appear, important issues regarding device stability remains, as well as the requirement for the use of non-heavy and non-toxic elements.[10] Therefore, research efforts in the field of conventional dye-sensitized cells remain crucial, such as the quest for efficient sensitizers that cover a large fraction of the solar spectrum. In this context, several studies focus on the development of alternative organic or inorganic dyes, as well as on the use of advanced concepts for efficient photon harvesting.[11] Among these concepts, the use of antennas that can harvest some complementary regions of the solar spectrum was shown to be a relevant strategy,[12] as recently reviewed in the literature.[13] The role of the antenna is to transfer its photonic excitation to the injecting sensitizer *via* an energy transfer step, leading to an extended response of the device. Energy transfers occur generally through two main mechanisms:[13] the long-range Förster resonant energy transfer (FRET),[14] which is a coulombic mechanism involving mainly two singlet states, and the Dexter process,[15] which is a short range double electron exchange between the donor and the acceptor. In general, for an efficient energy transfer, the lowest excited state of the antenna must be higher than that of the injecting dye. Efficient energy transfers are therefore much easier to achieve with low lying excited state of red or near infrared absorbing sensitizers than those having absorption bands spanning only in high energy region of the visible spectrum. Concerning solid-state DSSC, there are only few reports in the literature describing the use of antenna effect. The first reports were devoted to the use of ruthenium sensitizers bearing donor-antenna groups that exhibit multistep charge transfer cascades.[16, 17] Another strategy was based on a phosphorescent

relay dye mixed within the matrix of the solid-state organic HTM such as spiro-OMeTAD, exploiting efficient Förster energy transfers from unbound antennas located in the surrounding of the TiO_2/dye interface to the sensitizers.[18, 19] More recently, conjugated polymers acting as HTM within ssDSSC devices have also been observed playing a role of antennas that contribute to photocurrent generation.[20] In the two latter cases, the active antenna compound is played by the entire HTM, or mixed within the whole HTM phase, so that a large fraction of antennas does not efficiently transfer their excitation to the injecting dye. To address this issue, an advanced strategy is to exploit supramolecular interactions between antenna molecules and the injecting dye grafted at the TiO_2 surface, through rational molecular design. Several demonstrations of the concept have been reported for liquid electrochemical cells,[21, 22] bulk heterojunctions,[23] and liquid DSSC,[24, 25] however, to the best of our knowledge, there is no application of supramolecular assemblies to solid-state DSSC yet.

Herein, we report on the implementation of a supramolecular assembly based on imidazole functionalized borondipyrromethene (BODIPY, referred as antenna A_1) appended *via* coordination bond to a bichromophoric sensitizer (dyad D) based on a zinc porphyrin linked to a squaraine unit. This system has been successfully applied on liquid DSSC, leading to the demonstration of efficient energy transfer from the antenna to the injecting squaraine unit, through a multistep energy transfer cascade.[25] The spectral coverage of the dyad was broadened by the contribution of the antenna in the 450-550 nm range, and as a consequence, the photocurrent was significantly improved in the presence of the antenna (20% increase). However, inherent dye desorption mechanisms, leading to the presence of a slight fraction of antenna in the electrolyte, limit the stability of the approach. Such drawbacks are expected to be addressed using a solid-state electrolyte. We thus describe the optical properties of the supramolecular assembly using steady-state and transient photoluminescence techniques, and the optoelectronic properties of ssDSSC. We have also investigated the possibility for the antenna to contribute to photocurrent generation by direct electron injection in TiO_2, without any participation of the dyad, and we found that this pathway has a marginal contribution to the overall current enhancement.

2. Experimental section

Dyad D and antenna A_1 have been synthesized using published procedures.[25, 26]

2.1 Dissolution of molecules in solution

For the optical characterizations in solution, dissolution of dyad D was performed in an ethanol:dichloromethane (Sigma-Aldrich) mixture (1:1 in volume) at 0.05 mg/ml. Antenna A_1 was solubilized at 0.006 mg/ml in acetonitrile (Sigma-Aldrich). The solutions were left for 30 min at 50 °C under stirring to achieve the complete dissolution of the molecules.

For the D/A_1 mixture in solution, an initial solution of A_1 was prepared as reported above. The initial concentration of molecule A_1 was 0.0125 mM (0.006 mg/ml). Then, a suitable volume of a solution of dyad D at 0.05 mg/ml in ethanol:dichloromethane (1:1 in volume) was added dropwise to the antenna solution, within subsequent steps, leading to a D/A_1 molar ratio ranging from 0 to 1.56, taking into account every dilution resulting from the addition of solution of dyad D.

2.2 Preparation of dye-sensitized porous TiO_2 electrodes

For the optical characterization of dye-sensitized porous TiO_2 electrodes, nanoporous TiO_2 electrodes were prepared on FTO glass substrates (Solaronix SA, Switzerland, 15 Ω/□) previously coated with a dense TiO_2 layer. This dense layer, which acts as a hole blocking layer, was deposited on pre-cleaned FTO substrates by chemical spray pyrolysis, following a recipe previously published.[27] After a short UV ozone treatment, porous TiO_2 layers were deposited by spin-coating from a commercial TiO_2 paste (Dyesol, Australia) diluted at 50% with absolute ethanol. The resulting layers were then gradually sintered up to 450 °C for 45 min in air, before applying a conventional $TiCl_4$ treatment and final sintering at 500 °C.[27] The resulting electrodes show a thickness of 2 μm. They were then soaked in diluted solutions of dyad D (0.2 mM in an ethanol:dichloromethane mixture, 1:1 in volume, soaking performed at 70 °C in the dark and overnight), or antenna A_1 (0.2 mM in acetonitrile, soaking performed at room temperature overnight). It is worth noting that dyad D was always associated with deoxycholic acid (DCA) as co-adsorbant in order to prevent from molecule aggregation, as reported in a related study on liquid DSSC.[25] All the substrates were rinsed after the soaking step, using the same solvent used for the sensitization. The supramolecular assembly of A_1 on D was performed by soaking the D-sensitized electrode in the A_1 diluted solution at room temperature and for 1 h in order to prevent the desorption of dyad D.

2.3 Device fabrication

ssDSSC devices were prepared using reported procedures.[27] Briefly, the porous TiO_2 electrodes sensitized with the chromophores are infiltrated under ambient conditions by the molecular hole conductor 2,2',7,7'-tetrakis(N,N-dip-methoxypheny-amine)-9,9'-spirobifluorene (spiro-MeOTAD, Merck KGaA, Germany) from spin-coating, using conventional recipes with lithium

salt and *tert*-butylpyridine as additives.[27] Silver top electrodes were finally evaporated under *vacuum* (10^{-6} mbar) using shadow masks that define two active areas per substrates (0.18 cm^2 each).

2.4 Characterization techniques

Optical properties of solutions and films were recorded in transmission using a SAFAS DES200 spectrometer. Steady-state photoluminescence spectra were recorded using a FLS980 spectrometer (Edinburgh Instruments, UK). The excitation was provided by a monochromated 450W Xenon lamp and the detection was made in the 200-870nm range by a cooled R928P Hamamatsu photomultiplier (dark count <50 cps). Liquid samples were analyzed using quartz cuvettes in a 90° geometry. Solid-state samples were placed in a specific sample holder, using a 45° geometry. Slit widths were adjusted to maximize the signal to noise ratio, leading to a spectral bandwidth of 1.5 nm approximately. PL lifetimes were measured on the same apparatus, using time correlated single photon counting (TCSPC) and a picosecond diode laser at 509 nm as excitation source (temporal width of 150 ps). The instrument response function was measured for each sample using a diffusive reference sample. Current density-voltage characteristics were recorded in air using a calibrated Keithley 2400 source-measure unit, in the dark and under simulated solar emission provided by a 1600W NEWPORT solar simulator equipped with an AM1.5G filter. The spectral mismatch between the emission of the solar simulator and the standard AM1.5G (ASTM G173-03) solar spectrum was taken into account using standard procedures[28] and the solar simulator irradiance was corrected accordingly to match 100 $mW.cm^{-2}$ on the tested cells. The incident photon to charge carrier efficiency (IPCE) was obtained by a monochromated 75W Xenon lamp (Newport) and a calibrated pico-ammeter. The absolute IPCE is estimated using a calibrated certified Si photodiode of known spectral response.

3. Results and discussion

3.1 Properties of the chromophores in solution

The chemical structure of dyad D and antenna A_1 are presented in Figure 1. Their optical properties in solution, including UV-vis absorption and photoluminescence (PL), are presented in Figure 2. These data are in agreement with those previously reported for the molecules in solution.[25]

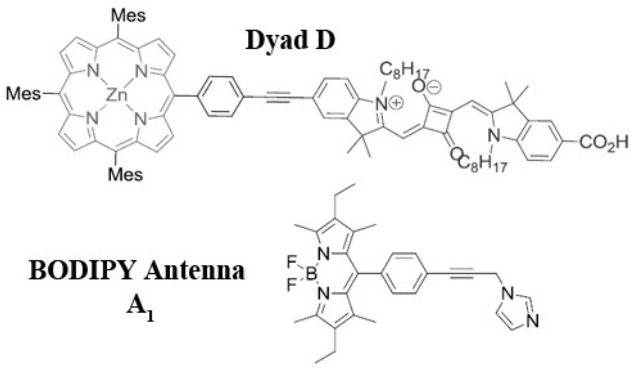

Figure 1 – Chemical structure of dyad D and BODIPY antenna A_1.

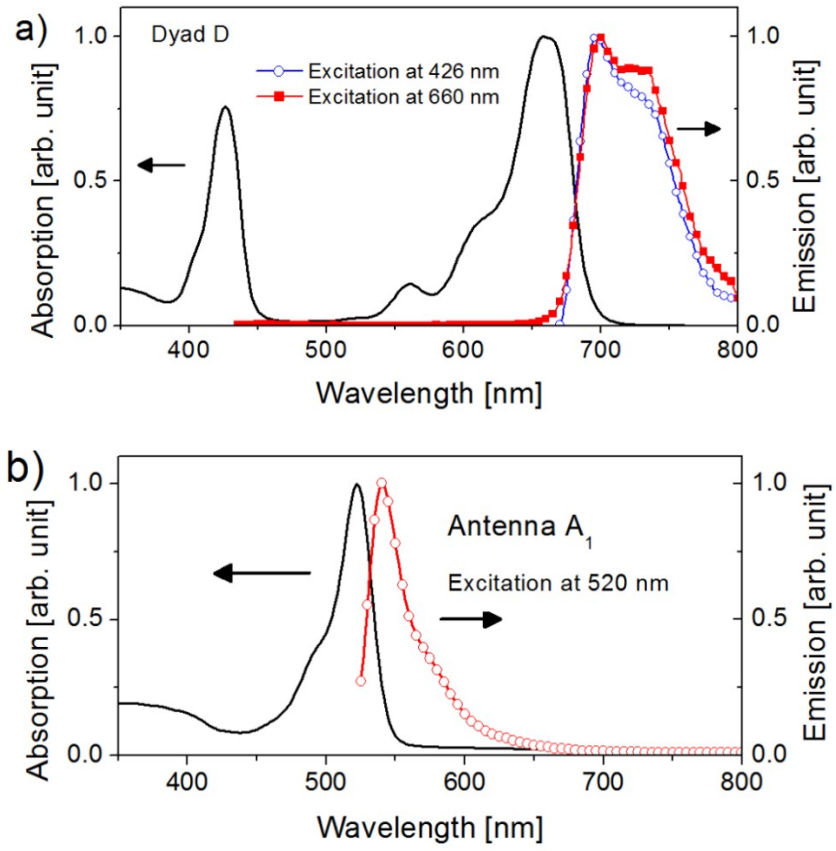

Figure 2 – Optical absorption (black solid line) and steady-state photoluminescence of (a) dyad D (ethanol:dichloromethane mixture, 1:1 in volume) for different excitation wavelengths: 426 nm (open circles) and 660 nm (solid squares), and (b) antenna A_1 in acetonitrile.

Dyad D is a bichromophoric species where both porphyrin and squaraine units are linked with a π-conjugated bridge. However, the groups are found to be almost independent due to the anti-periplanarity of the porphyrin and the phenyl. Consequently, the specific absorption bands of both units are clearly visible in the absorption spectrum of the dyad (Figure 2a). The Soret and Q-bands of the zinc porphyrin are easily observed at 426 nm and 560/600 nm respectively, as well as the clear contribution of the squaraine in the red part of the spectrum (600-700 nm). The

shoulder at 615 nm is associated with vibronic contributions. Clearly, excitation of either the porphyrin or the squaraine unit results in the squaraine emission only, indicating that a quantitative intramolecular energy transfer is occurring between the porphyrin to the squaraine. The antenna absorption around 500 nm nicely completes the 450-550 nm region where the dyad is transparent. Moreover, the emission spectrum of antenna A_1 significantly overlaps with the absorption spectrum of the dyad, which is a required condition for efficient energy transfer by Förster mechanisms. The energy transfer from the antenna to the dyad was first investigated in solution, by monitoring the emission of a D:A_1 mixture for various D/A_1 molar ratios ranging from 0.04 to 1.56, upon selective excitation of the antenna (Figure S1, ESI). We clearly observe an increase of the squaraine emission as the concentration of the dyad increases, accompanied by a decrease of the antenna emission. As the dyad does not absorb at the excitation wavelength, this observation clearly shows that the enhanced emission intensity is due to an energy transfer from the antenna to the dyad. However, the quenching of the antenna emission is only partial, even when there is an excess of dyad D with respect to the antenna molecules, suggesting that supramolecular interactions remain weak in these experimental conditions. In particular, the antenna was initially dissolved in an ethanol:dichloromethane mixture, which is suitable to properly dissolve the dyad, but which is not the best choice to solubilize the antenna. Some aggregation is therefore likely to occur in the solution. We note that this partial quenching of the antenna emission is associated with a very slight decrease of its PL lifetime, from 4.62 ns for a pure solution of A_1 to 4.56 ns for the mixture corresponding to a D:A_1 molar ratio of 1.56 (Figure S2, ESI). In fact, as the fraction of antenna bound to the dyad is likely to be low in solution, this shorter lifetime is likely to result from the coexistence of a majority of free antenna molecules presenting a long decay lifetime with a minority of bound antenna of shorter lifetime. The reduced lifetime observed here might thus indicates that efficient energy transfers are occurring between the bound antenna and the dyad.

3.2 Properties of the chromophores on TiO_2

We then prepared mesoporous TiO_2 electrodes deposited on FTO glass substrates and coated with the dyes in order to evaluate the optical properties of the grafted dyad in the presence of the A1 antenna. To this end, the porous electrodes are first soaked in a diluted solution of dyad D in the presence of deoxycholic acid (DCA) before being rinsed, and dipped in a second solution containing antenna A_1 alone. A final rinsing step is then performed. Such a procedure was found to induce the self-assembly of the antenna molecules at the TiO_2/D surface, due to the axial coordination occurring between the imidazole moiety and the zinc porphyrin, leading

to efficient Förster energy transfer.[25] In this study, we have also investigated the properties of TiO_2 electrodes sensitized by the antenna alone, in order to evaluate if efficient electron injection can occur from the antenna to the TiO_2. In this case, the presence of the antenna in the vicinity of TiO_2 could provide a second path for charge generation in the solar cells. The optical density of our 2-μm thick sensitized electrodes are presented Figure 3.

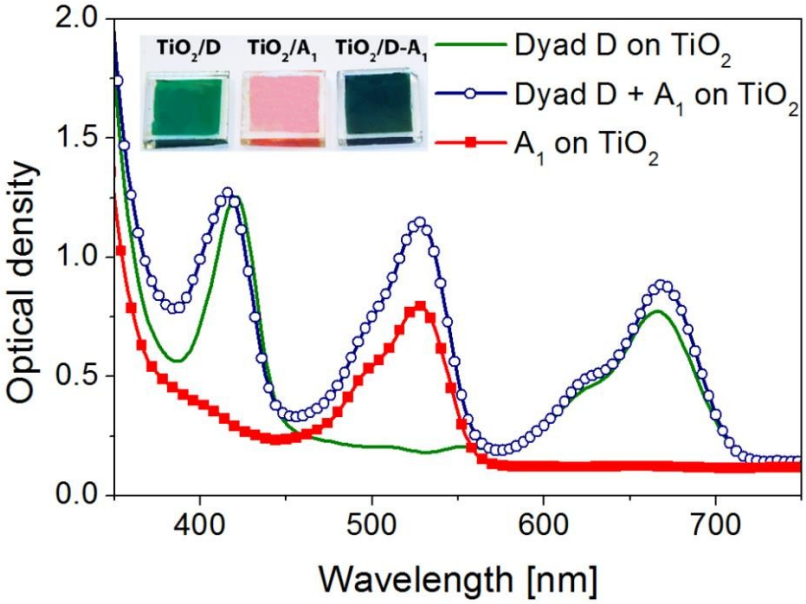

Figure 3 – Optical absorption spectra of the chromophores on 2-μm thick TiO_2 electrodes: dyad D (solid line), dyad D and antenna A_1 supramolecular assembly (open circles), and antenna A_1 alone (solid squares). The inset presents a photography of the sensitized electrodes.

The D- and D-A_1-sensitized electrodes show the expected optical contributions of dyad D and BODIPY antenna. A broadening of the squaraine bands is also observed, as well as a bathochromic shift of the contributions with regard to the spectra in solution. This shift is usually associated with a coupling between the π* states of the squaraine unit with the 3d orbitals of TiO_2. Also, we observe an intense band at 610 nm which can be associated with the presence of H-aggregates of the squaraine unit.[29] This band is usually indicative of a plan-to-plan aggregation of the molecules, leading to an excited state of higher energy. Additional effects of this aggregation are also evidenced through the broadening of the Soret band of the porphyrin unit.[30, 31] The presence of the antenna is clearly revealed in the spectrum of the sample combining the two chromophores, leading to a panchromatic response of the electrodes. No significant desorption of dyad D following the soaking step in the solution of antenna A_1 was observed, suggesting that the experimental conditions used for solid-state devices (use of thinner TiO_2 electrodes mainly) are slightly more favorable than that used in liquid DSSC

devices.[25] In particular, such desorption of the dyad in a liquid environment is a specific drawback of liquid cells that is expected to be addressed using a solid-state electrolyte. More interestingly, going back to the optical properties of the chromophores on TiO_2, the supramolecular assembly of antenna A_1 on dyad D is clearly evidenced as we observe the characteristic shifts of the Soret ($\Delta\lambda$ = 5nm) and Q ($\Delta\lambda$ = 15nm) bands of the zinc porphyrin unit, which indicate a coordination on the zinc atom,[32] as reported in the case of thicker TiO_2 electrodes devoted to liquid DSSC.[25] Interestingly, the antenna alone is also adsorbed at the surface of TiO_2, even after a quick rinsing step, despite the fact that no carboxylic acid anchoring group is present. This is certainly driven by hydrogen or coordination bonding of the nitrogen of imidazole to TiO_2, as it was previously shown with pyridyl anchor.[33-35] The absolute optical density of the film at 520 nm is only slightly lower than that of the D-A_1 supramolecular assembly on TiO_2, indicating that a quite significant amount of antenna molecule can also be adsorbed on the TiO_2 surface without the dyad. The slight increase of the absorbance of the shoulder at 500 nm could however indicate a slight aggregation of the molecule at the surface. In any case, TiO_2/antenna interfaces are likely to contribute to charge generation as well, even in systems based on D-A_1, if free spaces are left in between the chemisorbed dyad molecules. Further information on this aspect was obtained through photoluminescence spectroscopy. Figure 4 presents the steady-state photoluminescence spectra of the various chromophoric systems on TiO_2, recorded at various excitation wavelengths.

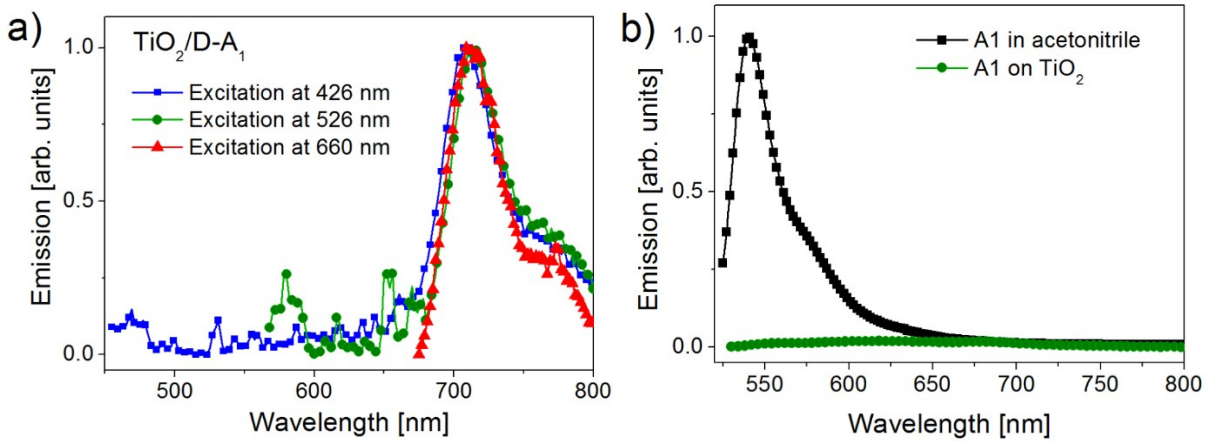

Figure 4 – Steady-state photoluminescence spectra recorded on TiO_2 for (a) the supramolecular assembly D-A_1 for various excitation wavelengths and (b) antenna A_1 alone in solution and on TiO_2. In this latter case, the spectra are normalized to the optical absorption of the antenna at 520 nm where the excitation is performed.

The dyad D alone on TiO_2 excited either at 426 nm or 660 nm exhibits a small but detectable emission of the squaraine unit at 706 nm (Figure S3, ESI). This emission was also observable for the supramolecular assembly of D-A1 on TiO_2 (Figure 4a). The intensity of this squaraine emission is however highly quenched as revealed by the high signal-to-noise ratio, indicating that an efficient electron injection occurs from the dyad to TiO_2, as expected. The observation of a remaining emission is likely to indicate that the TiO_2/D interface is still not optimal as some unquenched dyes remain on the TiO_2 surface. In any case, the emission of the porphyrin unit is completely quenched, as seen from the excitation at 426 nm, because the squaraine emission is the only contribution in the emission spectra. Once again, this indicates a quantitative energy transfer from the porphyrin to the squaraine, as observed in solution. When the antenna is bound on the dyad through supramolecular interaction (Figure 4a), we still observe the only contribution of the squaraine emission. Considering the high photoluminescence yield of BODIPY compounds and the high optical density (~1) of the film at 526 nm, this observation is consistent with a quantitative energy transfer from the A_1 antenna to the grafted sensitizer. As far as the emission properties of the antenna itself is concerned, we have determined that upon adsorption on TiO_2, a significant emission quenching (93%) occurs relative to that in solution (Figure 4b). In parallel, we compared the PL lifetime of the antenna in solution and on TiO_2 (Figure 5a).

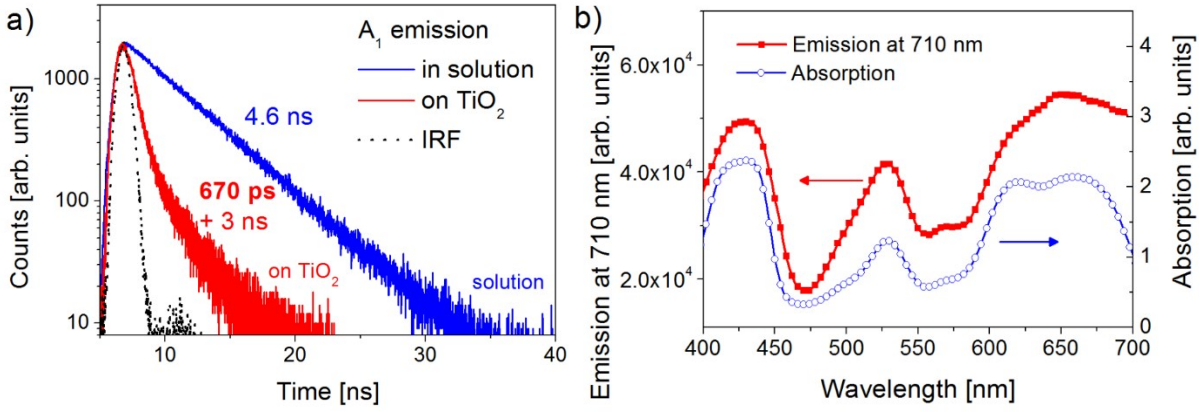

Figure 5 – (a) PL decays of antenna A_1 in solution (acetonitrile, 0.0125 mM) and adsorbed on a TiO_2 film. The excitation is performed at 509 nm and the emission is detected at 616 nm. (b) Excitation spectrum of the D-A_1 supramolecular assembly on TiO_2 (emission at 710 nm) compared to the optical absorption of the film.

The PL decay of the molecule on TiO_2 is drastically altered compared to the solution. The deconvolution of the spectrum, taking into account the instrument response function (IRF), shows a bi-exponential decay with a main population decaying within 670 ps only, and a second

population decaying within approximately 3 ns. These observations are consistent with an efficient charge transfer occurring between the antenna and the metal oxide electrode. Such mechanism can thus contribute to charge generation in the devices. Considering the energetic cascade evidenced for the supramolecular assembly, radiative energy losses could therefore be mainly attributed to the decay of squaraine excited states for a small fraction of molecules which are not optimally positioned at the TiO_2 surface. Our data suggest that the antenna can efficiently transfer its excitation energy to the dyad through energy transfer, or can quite efficiently inject an electron into the TiO_2 if it comes in its close vicinity.

Finally, the excitation spectrum of the supramolecular assembly of dyad D and antenna A1, monitored at the squaraine emission at 710 nm, exhibits a close match with its optical absorption, indicating that energy transfer is a major deactivating pathway on TiO_2.

3.3 Photovoltaic performance of solid-state dye-sensitized solar cells

The sensitized porous TiO_2 electrodes were finally infiltrated using the reference spiro-OMeTAD HTM, following a conventional methodology.[27] The HTM was doped with lithium salt and *tert*-butylpyridine, and processed using a standard spin-coating cycle in ambient conditions.[36, 37] The infiltration step is particularly crucial in the context of the supramolecular assembly, as it can affect the stability of the bonding between the dyad and the antenna. The optical properties of the HTM-infiltrated electrodes were monitored using UV-visible transmission (Figure 6). The spectra corresponding to device electrodes sensitized using D or A_1 alone are presented in Figure S4 (ESI).

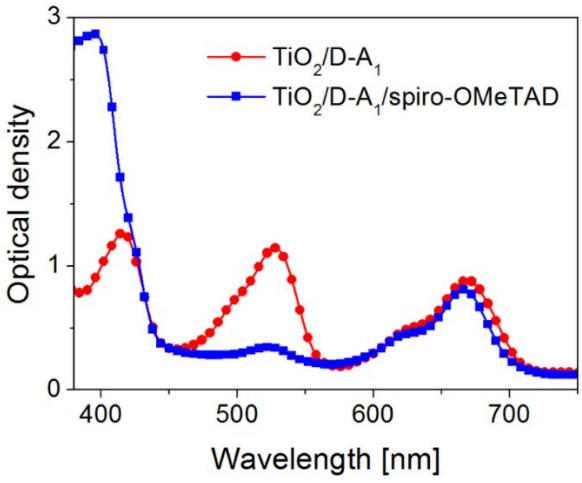

Figure 6 – UV-visible transmission spectra of porous TiO_2 electrode sensitized using the D-A_1 supramolecular assembly, before (red solid circles) and after (blue solid squares) the HTM infiltration.

We can observe a strong decrease of the contribution of the BODIPY group associated with the antenna after infiltration by the HTM, indicating that an important fraction of the antenna was removed during the spin-coating cycle of the spiro-OMeTAD solution. To better quantify the desorption of the dyes following the HTM infiltration, we estimated their apparent concentrations at the TiO_2 surface using the optical densities of the sensitized films, applying a simple Beer-Lambert's law as a first approximation (Table 1).

Table 1 - Apparent concentration of dye molecules adsorbed on TiO_2 (2 μm thick) for dyad D alone, D-A_1 supramolecular assembly, and antenna A_1 alone, before and after electrode infiltration by the HTM (spiro-OMeTAD). The maximum absorption wavelengths (λ_{max}) and corresponding molar extinction coefficients (ε) of the involved absorbing chemical groups are those obtained from the molecules in solution.[38]

Sample	chromophore	λ_{max} [nm]	ε at λ_{max} [$M^{-1}cm^{-1}$]	Effective concentration of adsorbed dye on TiO_2 [$mol.cm^{-3}$]		Fraction of molecules desorbed by the HTM
				No HTM	HTM	
TiO_2/D	Squaraine	664	$1{,}72.10^5$	$2{,}52.10^{-5}$	$2{,}49.10^{-5}$	-1%
TiO_2/D-A_1	Squaraine	664	$1{,}72.10^5$	$2{,}79.10^{-5}$	$2{,}58.10^{-5}$	-7%
TiO_2/D-A_1	BODIPY	526	$5{,}30.10^4$	$1{,}19.10^{-4}$	$3{,}56.10^{-5}$	-70%
TiO_2/A_1	BODIPY	526	$5{,}30.10^4$	$8{,}28.10^{-5}$	$3{,}56.10^{-5}$	-57%

Clearly, the spin-coating cycle used for spiro-OMeTAD infiltration washes a significant amount of antenna molecules, both for sample based on the supramolecular assembly of D with A_1 and for sample based on the antenna alone. This is unsurprising as the spin-coated solution of spiro-OMeTAD contains *tert*-butylpyridine, which can act as a competitive ligand to imidazole for the axial ligation onto zinc porphyrin. This re-solubilization of antenna molecules is less surprising for A_1 alone on TiO_2 considering that no anchoring groups are present in this case. No significant desorption of dyad D alone is evidenced, only a slight re-solubilization is observed in the case of the supramolecular assembly, in accordance with the fact that an additional dipping step of the D-sensitized electrode in the antenna solution is used in this case. We finally note that a larger amount of antenna molecules are present in the electrode in the presence of dyad D compared to sample based on A_1 alone, which is consistent with the supramolecular interactions occurring in this case.

The infiltrated sensitized-electrodes were finally completed by the deposition of silver top contacts, leading to working ssDSSC devices. The current density-voltage characteristics of the

cells are presented in Figure 7a, and the corresponding photocurrent action spectra, or incident photon to charge carrier efficiency (IPCE), are reported in Figure 7b. The extracted photovoltaic parameters are summarized in

Modest photovoltaic performance is observed for dyad D alone. Compared to liquid DSSC,[25] the short-circuit current density (JSC) is found significantly reduced by a factor of four, which can be mainly be attributed to the reduction in the electrode thickness for solid-state devices, leading to a lower light harvesting efficiency of the active layer.

Table 2.

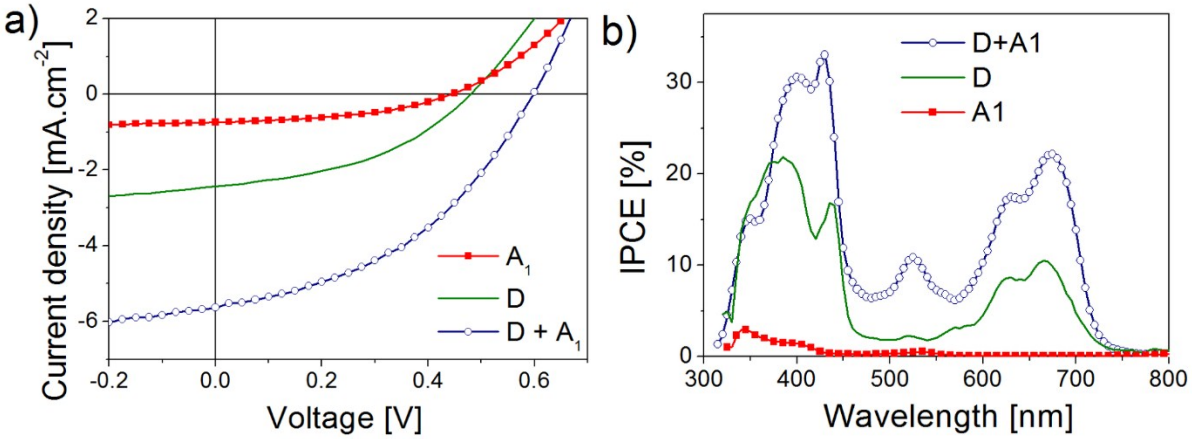

Figure 7 – (a) Current density/voltage characteristics under simulated sunlight (AM1.5G, 100 mW.cm^{-2}) of ssDSSC devices based on the different molecules. (b) Corresponding photocurrent action spectra.

Modest photovoltaic performance is observed for dyad D alone. Compared to liquid DSSC,[25] the short-circuit current density (J_{SC}) is found significantly reduced by a factor of four, which can be mainly be attributed to the reduction in the electrode thickness for solid-state devices, leading to a lower light harvesting efficiency of the active layer.

Table 2 - Photovoltaic parameters of ssDSSC devices under simulated solar emission (AM1.5G, 100 mW.cm^{-2})

	V_{OC} [mV]	J_{SC} [mA.cm^{-2}]	FF	η [%]
Dyad D	475	2.42	0.43	0.49
Dyad D + Antenna A_1	593	5.58	0.43	1.42
Antenna A_1	436	0.73	0.45	0.14

In addition, for dyad D alone, both the open-circuit voltage (V_{OC}) and fill factor (FF) are found significantly reduced in the solid-state devices, leading to a poor photoconversion efficiency of 0.49%. This observation suggests that some optimizations of the experimental conditions are indeed required for solid-state devices with respect to those used for liquid cells. The supramolecular association of the sensitizer with antenna A_1 induces a drastic improvement in photocurrent, as well as in open-circuit voltage, resulting in a huge gain of the overall performance of the cell by a factor of nearly three (Table 2). The IPCE spectrum of the device bearing the supramolecular assembly evidences two important features compared to the spectrum of dyad D alone. First, an additional contribution centered at 526 nm is observed. This contribution matches well the absorption band of the antenna, evidencing that it efficiently contributes to photocurrent generation. This photo-generation can result either from efficient energy transfer to the squaraine unit or from the direct injection of electrons from the antenna to TiO_2, as mentioned in the previous section. We note that this latter effect would require an efficient regeneration of the neutral state of the antenna by the solid-state HTM, so that an additional photocurrent can be extracted. However, inspection of the photovoltaic performance of the antenna alone adsorbed on TiO_2 demonstrates the generation of a rather poor photocurrent of less than 1 $mA.cm^{-2}$, in agreement with previous studies on liquid DSSC with BODIPY antenna.[25] It is also worth noting that BODIPY derivatives have been found to achieve quite poor performance in ssDSSC,[39] even in the presence of suitable anchoring groups. In the case of our BODIPY antenna, even lower efficiency is expected considering the weak binding of the molecule to the TiO_2 surface, as evidenced by the strong removal of antenna molecules after HTM infiltration. Therefore, the increase of IPCE in the 450-550 nm region is attributed to an efficient antenna effect occurring through the supramolecular assembly of A_1 with dyad D. As a result, the main effect of the A_1 species is to fuel the dyad with photonic energy, which improves the overall light harvesting efficiency of the device.

The second feature revealed by the IPCE spectrum in the presence of the supramolecular assembly is a significant improvement of charge generation over the entire spectral coverage of the sensitized electrode, compared to device based on dyad D alone. This indicates that the photo-generation due to dyad D is also nicely improved through the presence of the antenna. This observation is likely to be also related to the significant improvement of V_{OC} observed for the device. Several effects can be inferred to account for these observations. The presence of the antenna and its interactions with the dyad (axial ligation onto the zinc) can alter the configuration of dyad molecules at the TiO_2 surface. Such effect, although difficult to properly

address as the characterization of the local configuration at the interface is difficult, usually induces large variations in electron injection rates (ϕ_{inj}).[40, 41] ϕ_{inj} being one of the most important parameters affecting charge generation in dye-sensitized solar cells, the influence of the antenna on the local organization of dyad molecules seems to be a crucial factor to explain the improved charge generation by D in the presence of A_1. Other studies reported a strong influence of dye aggregation on electron injection rates,[42, 43] which is in our case another evidence for this hypothesis. Therefore, our data suggest that the antenna can affect the local configuration of dyad D molecules at the TiO_2 surface, leading to a large improvement in electron injection in TiO_2. It is then worth noting that such effect would also modulate the rate of charge recombination across the TiO_2/D-A_1/HTM interface. Accordingly, the device based on the supramolecular assembly exhibits an improved open-circuit voltage, compatible with longer-lived free charge carriers and improved charge diffusion lengths. We also suppose that antenna molecules can shield the TiO2 surface from the solid-state electrolyte, reducing the probability for charge recombination. Considering the amplitude of such effects for our devices, further investigations will be carried out to better understand the relationship between the configuration of the interface and device photo-physics.

4. Conclusion

We successfully transposed the concept of supramolecular antenna to solid-state DSSC devices, using a BODIPY antenna associated with supramolecular interaction to a bichromophoric sensitizer. The optical characterizations, performed both in solution and at the surface of TiO_2 nanoporous electrodes, confirm that efficient resonant energy transfers occur between the antenna and the grafted dyad, leading to a panchromatic absorption of the assembly. Moreover, we have evidenced an efficient photoluminescence quenching of the antenna emission by TiO_2, consistent with the occurrence of a direct injection of electrons in TiO_2 from the antenna. Solid-state DSSC based on the molecular spiro-OMeTAD hole transporter show an impressive improvement in performance of the device based on the dyad when the antenna is self-assembled with the zinc porphyrin. The corresponding power conversion efficiency recorded under standard solar emission is multiplied by a factor of three, indicating that the antenna concept is a relevant strategy towards panchromatism. However, a strong desorption/disassembly of the antenna was induced during the deposition of the hole transporter medium (spiro-OMeTAD), suggesting that improved deposition conditions could potentially achieve even larger performance. In this study, we have also evidenced that the antenna is highly beneficial for the re-organization of the TiO_2/dyad/electrolyte interface, leading to an

improved electron injection yield of the dyad. This strategy underscores that association of antenna by supramolecular interactions represent a viable strategy to prepare better performing solid-state hybrid devices for photovoltaic energy conversion.

Acknowledgments

The author are thankful for financial support from the "Region Limousin" (thematic project EVASION) and the CNRS/INSIS Energy program (NOXOMIX project). This work was performed in the framework of the Energy & Environment thematic of the SIGMA-LIM Laboratory of Excellence. The authors wish to also thank CNRS and the ANR HABISOL (program Asyscol, n° ANR-08-HABISOL-002) for financial supports and COST CM1202 program (PERSPECT H2O).

References

1. B. E. Hardin, H. J. Snaith and M. D. McGehee, *Nat Photon*, 2012, 6, 162-169.
2. J. Burschka, A. Dualeh, F. Kessler, E. Baranoff, N.-L. Cevey-Ha, C. Yi, M. K. Nazeeruddin and M. Grätzel, *Journal of the American Chemical Society*, 2011, 133, 18042-18045.
3. A. Michaleviciute, M. Degbia, A. Tomkeviciene, B. Schmaltz, E. Gurskyte, J. V. Grazulevicius, J. Bouclé and F. Tran Van, *Journal of Power Sources*, 2014, 253, 230-238.
4. B. Xu, E. Sheibani, P. Liu, J. Zhang, H. Tian, N. Vlachopoulos, G. Boschloo, L. Kloo, A. Hagfeldt and L. Sun, *Advanced Materials*, 2014.
5. J. Kim, J. K. Koh, B. Kim, S. H. Ahn, H. Ahn, D. Y. Ryu, J. H. Kim and E. Kim, *Advanced Functional Materials*, 2011, 21, 4633-4639.
6. Q. B. Meng, K. Takahashi, X. T. Zhang, I. Sutanto, T. N. Rao, O. Sato, A. Fujishima, H. Watanabe, T. Nakamori and M. Uragami, *Langmuir*, 2003, 19, 3572-3574.
7. E. V. A. Premalal, N. Dematage, G. R. R. A. Kumara, R. M. G. Rajapakse, M. Shimomura, K. Murakami and A. Konno, *Journal of Power Sources*.
8. I. Chung, B. Lee, J. He, R. P. H. Chang and M. G. Kanatzidis, *Nature*, 2012, 485, 486-489.
9. N.-G. Park, *Materials Today*, 2014, in press, DOI: 10.1016/j.mattod.2014.1007.1007.
10. M. A. Green, A. Ho-Baillie and H. J. Snaith, *Nat Photon*, 2014, 8, 506-514.
11. J. Bouclé and J. Ackermann, *Polymer International*, 2012, 61, pp.355.373.
12. R. Amadelli, R. Argazzi, C. A. Bignozzi and F. Scandola, *Journal of the American Chemical Society*, 1990, 112, 7099-7103.
13. F. Odobel, Y. Pellegrin and J. Warnan, *Energy and Environmental Science*, 2013, 6, 2041-2052.
14. T. Forster, *Naturwissenschaften*, 1946, 33, 166-175.
15. D. L. Dexter, *The Journal of Chemical Physics*, 1953, 21, 836-850.
16. C. S. Karthikeyan, H. Wietasch and M. Thelakkat, *Advanced Materials*, 2007, 19, 1091-1095.
17. C. Y. Chen, N. Pootrakulchote, S. J. Wu, M. Wang, J. Y. Li, J. H. Tsai, C. G. Wu, S. M. Zakeeruddin and M. Grätzel, *Journal of Physical Chemistry C*, 2009, 113, 20752-20757.
18. J. H. Yum, B. E. Hardin, S. J. Moon, E. Baranoff, F. Nüesch, M. D. McGehee, M. Grätzel and M. K. Nazeeruddin, *Angewandte Chemie - International Edition*, 2009, 48, 9277-9280.
19. G. K. Mor, J. Basham, M. Paulose, S. Kim, O. K. Varghese, A. Vaish, S. Yoriya and C. A. Grimes, *Nano Letters*, 2010, 10, 2387-2394.

20. R. S. Santosh Kumar, G. Grancini, A. Petrozza, H. J. Snaith and G. Lanzani, 2012.
21. N. K. Subbaiyan, C. A. Wijesinghe and F. D'Souza, *Journal of the American Chemical Society*, 2009, 131, 14646-14647.
22. A. Nomoto and Y. Kobuke, *Chem. Commun.*, 2002, 1104-1105.
23. F. Silvestri, I. López-Duarte, W. Seitz, L. Beverina, M. V. Martínez-Díaz, T. J. Marks, D. M. Guldi, G. A. Pagani and T. Torres, *Chemical Communications*, 2009, 4500-4502.
24. N. K. Subbaiyan, J. P. Hill, K. Ariga, S. Fukuzumi and F. D'Souza, *Chemical Communications*, 2011, 47, 6003-6005.
25. J. Warnan, Y. Pellegrin, E. Blart and F. Odobel, *Chemical Communications*, 2012, 48, 675-677.
26. J. Warnan, F. Buchet, Y. Pellegrin, E. Blart and F. Odobel, *Organic Letters*, 2011, 13, 3944-3947.
27. H. Melhem, P. Simon, L. Beouch, F. Goubard, M. Boucharef, C. Di Bin, Y. Leconte, B. Ratier, N. Herlin-Boime and J. Bouclé, *Advanced Energy Materials*, 2011, 1, pp.908-916.
28. V. Shrotriya, G. Li, Y. Yao, T. Moriarty, K. Emery and Y. Yang, *Adv. Func. Mater.*, 2006, 16, 2016-2023.
29. J. H. Yum, S. J. Moon, R. Humphry-Baker, P. Walter, T. Geiger, F. Nüesch, M. Grätzel and M. D. K. Nazeeruddin, *Nanotechnology*, 2008, 19.
30. K. E. Splan and J. T. Hupp, *Langmuir*, 2004, 20, 10560-10566.
31. C. F. Lo, L. Luo, E. W. G. Diau, I. J. Chang and C. Y. Lin, *Chemical Communications*, 2006, 1430-1432.
32. Y. Kobuke, in *Non-Covalent Multi-Porphyrin Assemblies*, Springer, 2006, pp. 49-104.
33. A. J. P. Cardenas, B. J. Culotta, T. H. Warren, S. Grimme, A. Stute, R. Fröhlich, G. Kehr and G. Erker, *Angewandte Chemie International Edition*, 2011, 50, 7567-7571.
34. D. Daphnomili, G. Landrou, S. Prakash Singh, A. Thomas, K. Yesudas, B. K, G. D. Sharma and A. G. Coutsolelos, *RSC Advances*, 2012, 2, 12899-12908.
35. J. Lu, X. Xu, Z. Li, K. Cao, J. Cui, Y. Zhang, Y. Shen, Y. Li, J. Zhu, S. Dai, W. Chen, Y. Cheng and M. Wang, *Chemistry – An Asian Journal*, 2013, 8, 956-962.
36. J. Krüger, R. Plass, L. Cevey, M. Piccirelli, M. Grätzel and U. Bach, *Applied Physics Letters*, 2001, 79, 2085-2087.
37. A. Abate, T. Leijtens, S. Pathak, J. Teuscher, R. Avolio, M. E. Errico, J. Kirkpatrik, J. M. Ball, P. Docampo, I. McPherson and H. J. Snaith, *Physical Chemistry Chemical Physics*, 2013, 15, 2572-2579.
38. J. Warnan, Thèse de Doctorat de Chimie, Université de Nantes, 2012.
39. S. Kolemen, Y. Cakmak, S. Erten-Ela, Y. Altay, J. Brendel, M. Thelakkat and E. U. Akkaya, *Organic Letters*, 2010, 12, 3812-3815.
40. S. E. Koops, B. C. O'Regan, P. R. F. Barnes and J. R. Durrant, *Journal of the American Chemical Society*, 2009, 131, 4808-4818.
41. R. Katoh and A. Furube, *Journal of Photochemistry and Photobiology C: Photochemistry Reviews*, 2014, 20, 1-16.
42. L. Luo, C.-J. Lin, C.-Y. Tsai, H.-P. Wu, L.-L. Li, C.-F. Lo, C.-Y. Lin and E. W.-G. Diau, *Physical Chemistry Chemical Physics*, 2010, 12, 1064-1071.
43. K. R. Mulhern, M. R. Detty and D. F. Watson, *The Journal of Physical Chemistry C*, 2011, 115, 6010-6018.